IEEE Transactions on Nuclear Science, Vol. NS-32, No. 3, June 1985

TIMING ELECTRONICS

AND

FAST TIMING METHODS WITH SCINTILLATION DETECTORS

T. J. PAULUS
EG&G ORTEC
OAK RIDGE, TN 37830

I. SUMMARY

Time spectroscopy involves the measurement of the time relationship between two events. This paper reviews time pick-off techniques, practival time-pickoff circuits, and timing with scintillation detectors. A detailed comparison is made between leading-edge timing and constant-fraction timing. Typical timing resolution results are given for ^{60}Co.

II. INTRODUCTION

Time Spectroscopy involves the measurement of the time relationship between two events. A simplified block diagram of a typical time spectroscopy system is shown in Fig 1. A source of time related radiation illuminates both detectors. Each detector output is processed by a time-pickoff unit. One signal is designated the "Start" and the other signal the "Stop". The Stop is delayed some small amount of time to insure that the Time to Amplitude Converter (TAC) operates within its linear range. The output signal from the TAC is a pulse whose height is proportional to the time difference between the Start and the Stop signals. A histogram of the TAC output is displayed on the Multichannel Analyzer, MCA.

A timing coincidence spectrum typical for coincident gamma rays is shown in Fig 2. The shape of the timing spectrum is critically important in time spectroscopy. The timing resolution must be high (the timing peak must be very narrow) so that the time relationship between two closely spaced events can be measured accurately. also, the narrow width of the spectral peak must be maintained down to a small fraction of its maximum height to ensure that all truly coincident events are recorded. Two common figures of merit for a timing spectrum are its width at half-maximum, FWHM, and its width at tenth-maximum, FWTM.

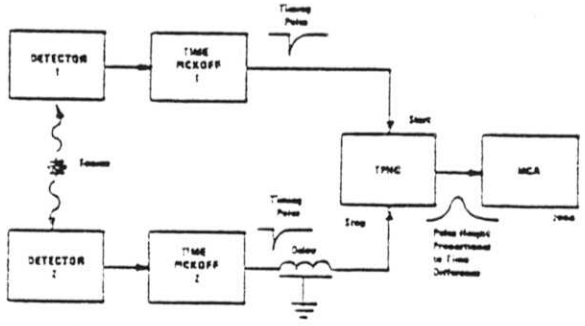

Fig 1. Simplified Block Diagram of a Typical Time Spectrometer.

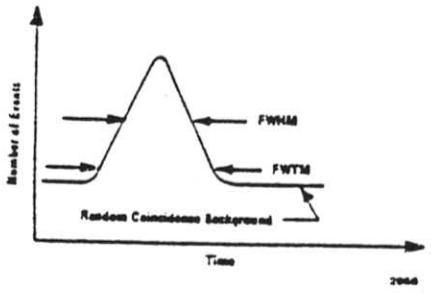

Fig 2. Timing Coincidence Spectrum.

III. TIME-PICKOFF TECHNIQUES

1. Time Derivation Errors

A particularly difficult problem in timing is to obtain a signal that is precisely related in time to the event. Some type of time-pickoff circuit is employed to produce a logic output pulse that is consistently related in time to the beginning of each input signal. Ideally, the time of occurrence of the logic pulse is insensitive to the shape and amplitude of the input signals.

There are three important sources of error in time-pickoff measurements: walk, drift and jitter. Walk is the time movement of the output pulse relative to the input pulse due to variations in the shape and amplitude of the input pulse. Drift is the timing error introduced by component aging and by temperature variations. Jitter is the time uncertainty that is caused by noise and by statistical fluctuations of the signals from the detector.

2. Leading Edge Timing

A leading-edge discriminator is the simplest means of deriving a time-pickoff signal. Using some form of comparator, a logic signal is produced when the input signal crosses a fixed threshold level. A primary disadvantage of this method is that the time of occurrence of the output pulse is a function of the amplitude and rise time of the input signal.

Time walk of a leading-edge comparator due to input signal variations is shown in Fig 3

0018-9499/85/0006-1242$01.00 ©1985 IEEE

In Fig 3, signals A and B have the same rise time but different amplitudes. Signal A crosses the threshold, V_{th}, at time t_1 while signal C crosses the threshold at time t_2. The difference in threshold-crossing time cause the output logic pulse from the leading-edge discriminator to "walk" along the time axis. Walk is most pronounced for signals with amplitudes that only slightly exceed the threshold level.

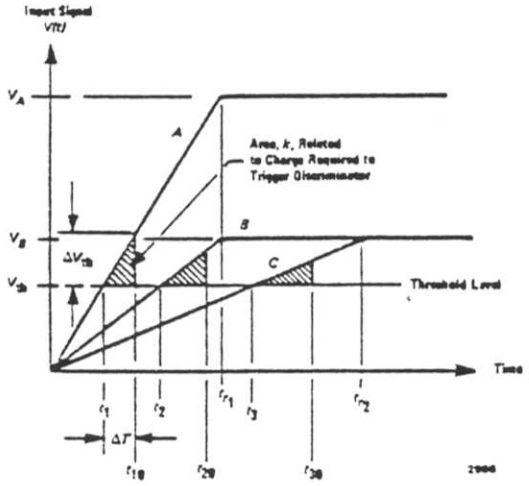

Fig 3. Walk in a Leading-Edge Discriminator Due to Amplitude and Rise Time Variations and Charge Sensitivity.

An additional contribution to the time walk of a real leading-edge discriminator is its charge sensitivity. Time walk due to charge sensitivity is also illustrated in Fig 3. After an input signal crosses the discriminator threshold level, a small additional amount of charge is required to actually trigger the discriminating element. Times t_{10}, t_{20} and t_{30} are the times when the output signals actually occur, relative to times t_1, t_2, and t_3. Timing errors introduced by charge sensitivity are greater for signals with longer rise times and for signals with smaller pulse amplitudes above threshold.

Charge sensitivity also introduces changes in the effective threshold level of the discriminator. For example, signal A in Fig 3 has an effective threshold of $V_{th} + \Delta V_{th}$. Effective threshold errors introduced by charge sensitivity are greatest for very narrow input signals. The specific characteristics of the input device also are a major factor in determining the charge sensitivity of the discriminator.

Jitter is another source of error in time-pickoff circuits. Noise can be present on the detector signal, be generated by the processing electronics, or can be generated by the discriminator itself. Statistical amplitude fluctuations cause an uncertainty in the time at which the signal crosses the discriminator threshold level.

Two sources of timing uncertainty are illustrated in Fig 4 for an ideal leading-edge discriminator. Assume a

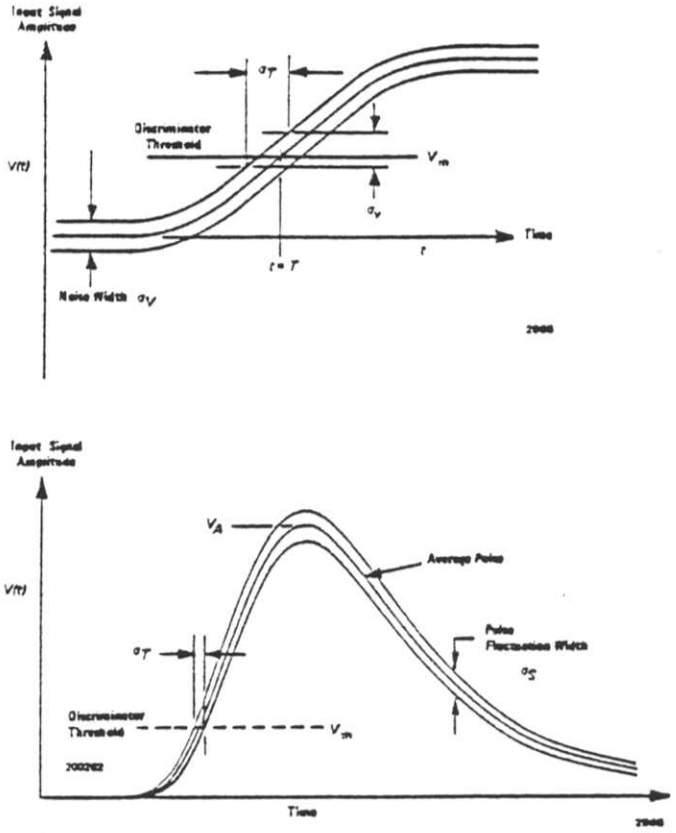

Fig 4. Time Jitter in a Leading-Edge Discriminator Due to (a) Noise on the Input Signal and (b) Statistical Pulse-Height Variations.

Gaussian-probability density of noise amplitude, with a zero mean, having a standard deviation (or RMS value) of σ_V. The noise-induced RMS uncertainty, σ_T, in threshold-crossing time for the leading-edge discriminator is given with reasonable accuracy by the triangle rule as

$$\sigma_T = \sigma_V / dV(t)dt|_{t=T} \qquad (1)$$

where the input signal V(t), is assumed to be approximately linear in the region of threshold crossing, and the discriminator threshold level is assumed to be removed from both the zero level and the peak level by at least the noise width. Timing jitter is inversely proportional to the slope of the input signal at threshold-crossing time. In general, signals with greater slopes at threshold-level crossing produce less time jitter.

When the leading-edge technique is restricted to those applications that involve a very narrow dynamic range of signals, excellent timing results can be obtained. Under these conditions timing errors due to charge sensitivity and to jitter are minimized for input signals with the greatest slope at threshold-crossing time. The best timing resolution is most frequently found by experimenting with the threshold level.

3. Constant Fraction Timing

The existence of of optimum triggering fraction for leading-edge timing with plastic scintillator/PMT systems stimulated the design of a circuit that would trigger at the optimum triggering fraction regardless of the input pulse height(2). Fig 5 shows a functional diagram of a constant fraction discriminator, CFD. In a CFD, the input signal is delayed and a fraction of the undelayed input is subtracted from it to produce a bipolar pulse. The zero crossing is detected and used to produce an output logic pulse. The use of a leading-edge arming discriminator provides energy selection capability and prevents the sensitive zero-crossing device from triggering on the noise of the constant-fraction baseline. A one-shot in series with the output circuit prevents multiple output signals from being generated from one input.

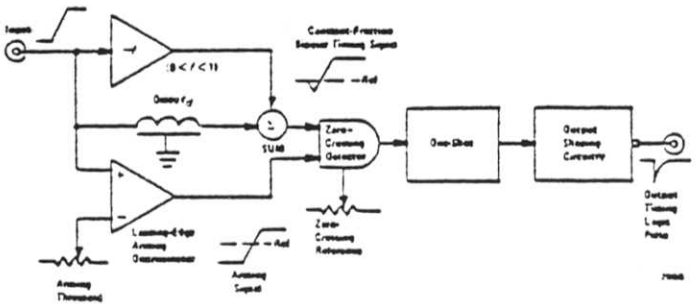

Fig 5. Functional Representation of a Constant-Fraction Trigger.

With the constant-fraction technique, walk due to rise time and amplitude variations of the input signal is minimized by proper selection of the shaping delay, t_d. Jitter is minimized by proper selection of the attenuation factor, f.

Two cases must be considered in determining the zero-crossing time of the constant-fraction bipolar signal. The first case if for true-constant-fraction (TCF) timing, and the second is for the amplitude-and-rise-time-compensated (ARC) timing(3).

In the TCF case the time of zero crossing occurs while the attenuated input signal is at its full amplitude. Fig 6 illustrates the signal formation in an ideal CFD for TCF timing with linear input signals. The amplitude independence of the zero-crossing time is depicted for input signals A and B which have the same rise time but different amplitudes. From signals B and C the zero-crossing time is seen to be dependent on the rise time of the input signal. For linear input signals that begin at time zero the constant-fraction zero-crossing time for the TCF case, T_{TCF}, is

$$T_{TCF} = t_d + ft_r \qquad (2)$$

where t_r is the input signal rise time.

Two criteria for t_d must be observed to ensure TCF timing. The shaping delay must be selected so that

$$t_d > t_r(1 - f). \qquad (3)$$

This constraint ensures that the zero-crossing time occurs after the attenuated linear input signal has reached its maximum amplitude. Practical timing experiments involve input signals with finite pulse widths; therefore the shaping delay must also be made sufficiently short to force the zero crossing signal to occur during the time that attenuated signal is at its peak.

TCF timing is most effective when used with input signals having a wide range of amplitudes but having a narrow range of rise times and pulse widths. these restrictions favor the use of TCF timing in scintillator/PMT systems. Any remaining walk effect can be attributed to the charge sensitivity of the zero-crossing detector and the slew limitations of the devices used to form the constant-fraction signal.

The second case to be considered is ARC timing, when the time of zero crossover occurs before the attenuated input signal has reached its maximum pulse height. This condition eliminates the rise-time dependence of the zero-crossing time that limits the application of the TCF technique. Fig 7 illustrates the signal formation in an ideal CFD for ARC timing with linear input signals. The amplitude independence of the ARC

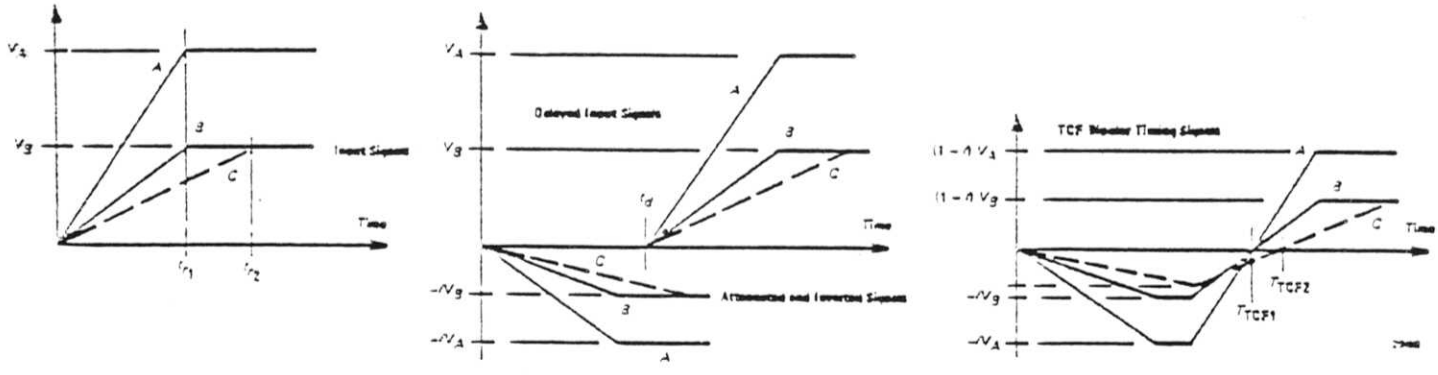

Fig 6. Signal Formation in a Constant-Fraction Discriminator for TCF Timing.

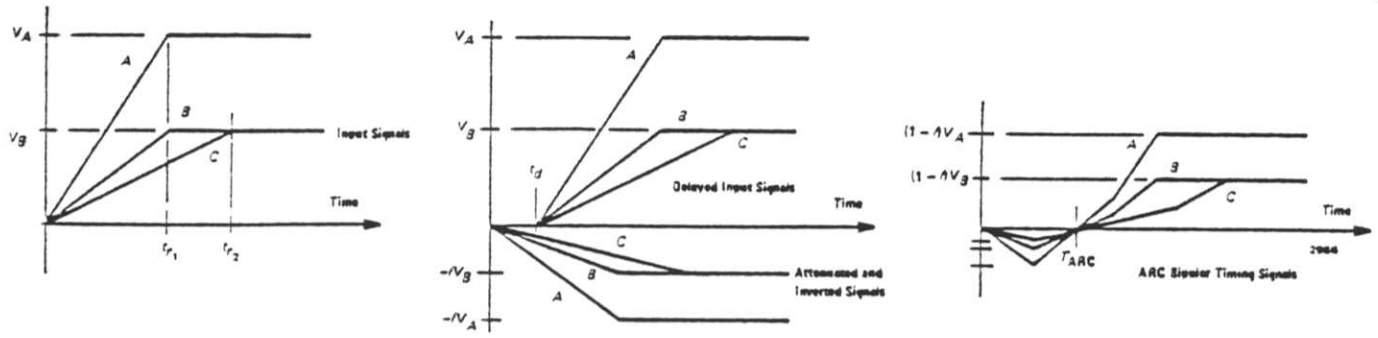

Fig 7. Signal Formation in a Constant-Fraction Discriminator for ARC Timing.

zero-crossing time is depicted for input signals B and C, which have the same amplitude but different rise times. For linear input signals that begin at time zero the zero-crossing time, T_{ARC} is

$$T_{ARC} = t_d/(1 - f). \quad (4)$$

One criteria for t_d to ensure ARC timing is

$$t_d < t_{r(min)}(1 - f) \quad (5)$$

where $t_{r(min)}$ is the minimum expected rise time for any input signal. This constraint ensures ARC timing for all linear input signals with rise times greater than $t_{r(min)}$ regardless of input pulse width.

In ARC timing the fraction of the input pulse height at which the time-pickoff signal is generated is not constant. The effective triggering fraction for each input pulse is related to the attenuation fraction by the input signal rise time. For linear input signals the effective ARC-timing triggering fraction is

$$f_{ARC(eff)} = ft_d/t_r(1 - f), \quad (6)$$

which is always less than f.

Analysis of the zero-crossing time jitter for linear input signals is outlined in Ref 1. For TCF timing,

$$\sigma_{T(TCF)} = \sigma_V(1 + f^2)^{1/2} / (V_A t_r); \quad (7)$$

for ARC timing,

$$\sigma_{T(ARC)} = \sigma_V(1 + f^2)^{1/2} / (V_A(1 - f)/t_r); \quad (8)$$

where V_A is the input signal amplitude and t_r is the input signal rise time.

A comparison between Eqs. (1), (7) and (8) leads to several interesting observations concerning noise induced jitter. Under identical input signal and noise conditions and for the same attenuation fraction, the jitter is usually worse for ARC timing than it is for TCF timing due to the more shallow slope of the ARC zero-cross signal. Under identical input and noise conditions, the jitter is usually worse for TCF timing than for leading-edge timing by the factor $(1 + f^2)^{1/2}$. However, TCF timing virtually eliminates time jitter due to statistical amplitude variations of the signals from the detector so that TCF timing often results in less overall jitter.

IV. PRACTICAL TIME-PICKOFF CIRCUITS.

The front-end of most timing instruments used in nuclear spectroscopy must process signals in the nanosecond range. The quality of these signals is very important in achieving state-of-the art timing results. Ringing and spurious signals are detrimental to good timing.

The circuit designer has an excellent array of active devices from which to choose. Both NPN and PNP transistors are available with values of f_T in excess of 5 GHz. A number of ECL logic circuits are available that can count in excess of 1 GHz. Several high-speed monolithic comparators are available. Tunnel diodes are still used in some critical applications because of their very low charge sensitivity and short rise time.

Some common problems still challenge the designer of fast circuits. Active device interaction with the circuit layout, stray lead inductance, body capacitance and unwanted signal coupling all place real limits on circuit performance. An equivalent circuit for an axial lead resistor is shown in Fig 8: Typical values for a 1/4 watt carbon composition resistor placed flush on a ground plane printed circuit board are 3 nH/cm and 0.3 pF/cm.

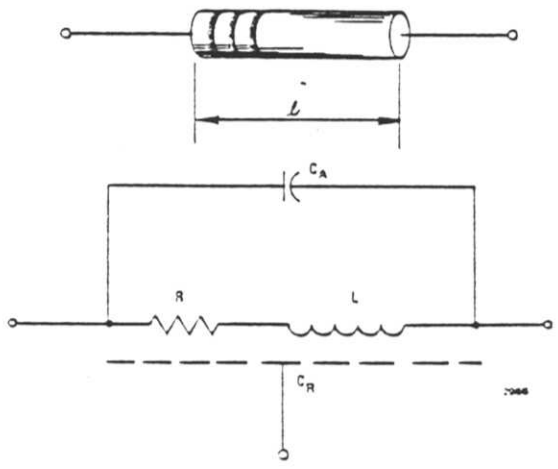

Fig 8. Equivalent Circuit for an Axial Lead Resistor.

The effect of these stray parameters are demonstrated by the simple circuit shown in Fig 9a. A fast transistor is switched off causing the 10 mA current to flow in the 10 ohm resistor. Fig 9b shows the transient waveform of the switching action measured with a sampling oscilloscope. The top trace in Fig 9b is for a 5%, 1/8 watt carbon composition resistor. The bottom two waveforms are for different types of 1% metal film resistors. All resistors had lead lengths less than 5 mm. The greatest overshoot is associated with the physically largest resistor. Fig 9c shows the effect of lead length for a 5%, 1/8 watt carbon composition resistor. The top waveform is for a 3 mm lead length, the middle waveform is for 23 mm lead length, and the bottom waveform is for 48 mm lead length. The longer the leads, the greater the spurious response. Due to the effects of various stray elements, the performance of many fact circuits is often determined by the art of the builder as well as the skill of the circuit designer.

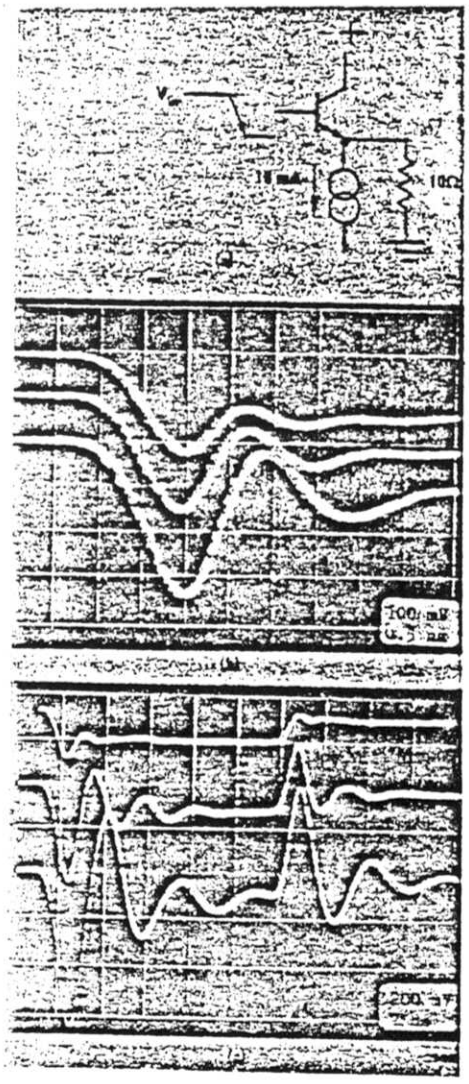

Fig 9. Transient Waveform Study (a) Simplified Circuit Diagram, (b) Different Resistor Types, and (c) Different Lead Lengths.

Many different circuits have been used to form the constant-fraction signal. The first CFD was built around a tunnel diode. Most modern CFD's use high speed monolithic comparators because of their speed and reliability.

The earlier discussion associated with Fig 3 described the principle functions that the constant-fraction circuit must perform. These included splitting the input signal, attenuating one part, delaying the other part, inverting either the delayed or the attenuated signal, summing the resulting signals, arming the zero-cross detector and detecting the zero-cross signal.

Two general circuits are used in modern CFD's. A block diagram of one type is shown in Fig 10a(4). The upper comparator is a leading-edge discriminator whose output arms the zero-crossing detector. The constant-fraction signal is formed actively in the input differential stage of the lower comparator. The monitor signal is taken at the output of the constant-fraction comparator which is typically an ECL logic level having an 800 mV signal range. Thus the monitor signal is clamped at about 400 mV peak-to-peak. The lowest threshold setting is approximately 5 mV and is determined by the characteristics of the leading-edge comparator.

The block diagram of a second and fundamentally different input circuit is shown in Fig 10b(5). In this circuit, the constant-fraction signal is formed passively in a differential transformer. The bandwidth of the transformer can be very high, >400 MHz. The monitor output is a close approximation of the actual constant-fraction signal since it is picked-off at the input to the constant-fraction comparator. The arming and zero-crossing detector circuits are the same as in Fig 10a. The minimum threshold is

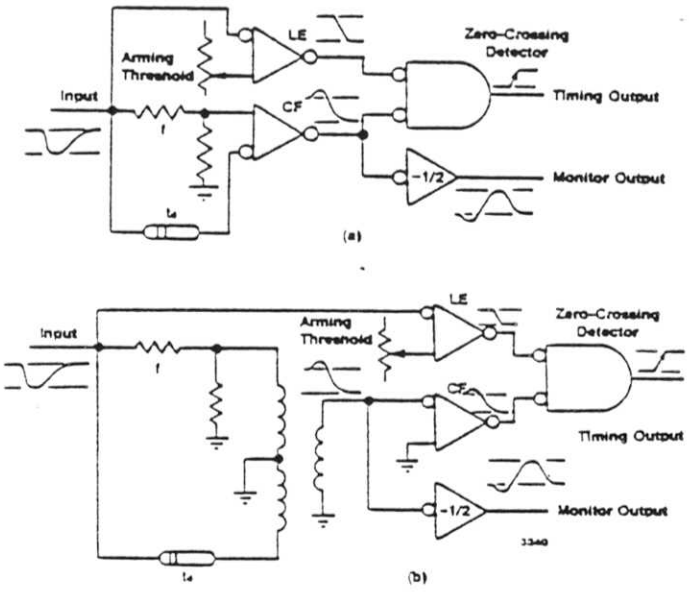

Fig 10. Two General Circuits used in Modern Constant-Fraction Discriminators.

about 30 mV due to the attenuation in the transformer resulting from maintaining a 50 ohm impedance level.

Most modern CFD's have provisions for adjusting the threshold level, the shaping delay and the walk. Some units allow adjustment of the fraction. A simple and useful test to insure that the CFD is properly adjusting is to view the monitor signal on a fast oscilloscope that is triggered by the output of the CFD. Because of the delay time through the CFD, it is usually necessary to delay the monitor signal.

Fig 11a shows the anode waveform of a typical scintillator/PMT system. Note the uniform rise times and the wide range of amplitudes. Fig 11b shows the monitor output of the CFD shown in Fig 10a. The well defined zero-crossing point indicates the quality of the CFD and its proper adjustment. Also note that the signal excursion is limited or clipped due to the limits on the output signal level of the ECL gate. Fig 11c shows the monitor output of the CFD shown in Fig 10b. The well defined zero-crossing point indicates the quality of the CFD and its proper adjustment. Also note that the signal excursion is not limited and that the entire constant-fraction signal is available for viewing.

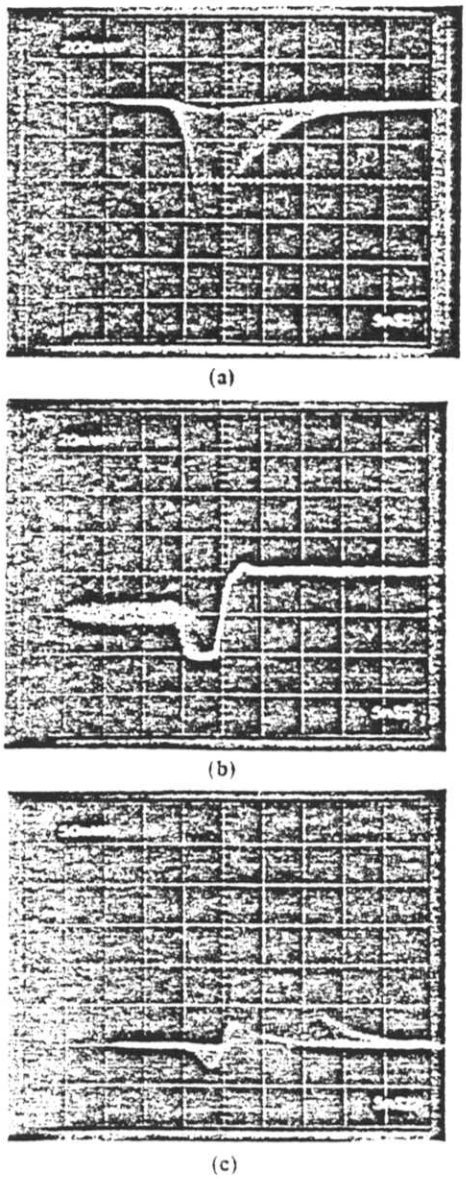

Fig 11. (a) Anode Waveform, (b) Monitor Waveform for CFD Shown in Fig 10a, (c) Monitor Waveform for CFD Shown in Fig 10b.

V. TIMING WITH SCINTILLATION DETECTORS

CFD's have been used in a wide variety of applications with fast plastic scintillators/PMT systems. One use, the Fast/Slow Timing System for Gamma-Gamma Coincidence Measurement, is shown in Fig 12. A CFD is associated with each detector and is referred to as the "Fast" or timing channel. Each detector also has a "Slow" or energy channel consisting of a preamplifier, shaping amplifier and timing single-channel analyzer, SCA. If the two energy channels are in coincidence, then the TAC is strobed and the resulting signal stored in an MCA. The Fast/Slow system has both excellent energy selection and timing characteristics. The only disadvantage of the Fast/Slow system occurs at high count rates since the TAC must handle all start-stop pairs regardless of their energy or coincidence.

Fig 13 shows a block diagram of the Fast Timing Coincidence System for Gamma-Gamma Coincidence Measurements. In this system, each CFD operates in the differential or SCA mode and generates both the timing information and selects the energy range of interest. If two detected events fall within the selected energy ranges, and if they are coincident within the resolving time set by the coincidence unit, the TAC is grated to accept the delayed Start and Stop input signals. Thus the TAC must handle start-stop pairs only for events that are of the correct energy and are coincident.

When operated at low count rates, less than 5 kc/s, both the Fast/Slow and the Fast timing systems give similar results(6). Fig 14 shows the timing resolution with ^{60}Co as a function of the dynamic range of the input signals. The FWHM timing resolution ranges from less than 200 ps at 1.1:1 dynamic range to less than 350 ps for 100:1 dynamic range. Data from the Fast and the Fast/Slow systems were within 5%.

VI. ACKNOWLEDGEMENTS

Special acknowledgement is due M.O. Bedwell who contributed greatly to the body of knowledge that formed the basis of this short course. Acknowledgement is also due the technical staff and management of EG&G ORTEC who encouraged and supported this work, to J. Halsey who typed the manuscript, and to J. Schall who prepared the final copy.

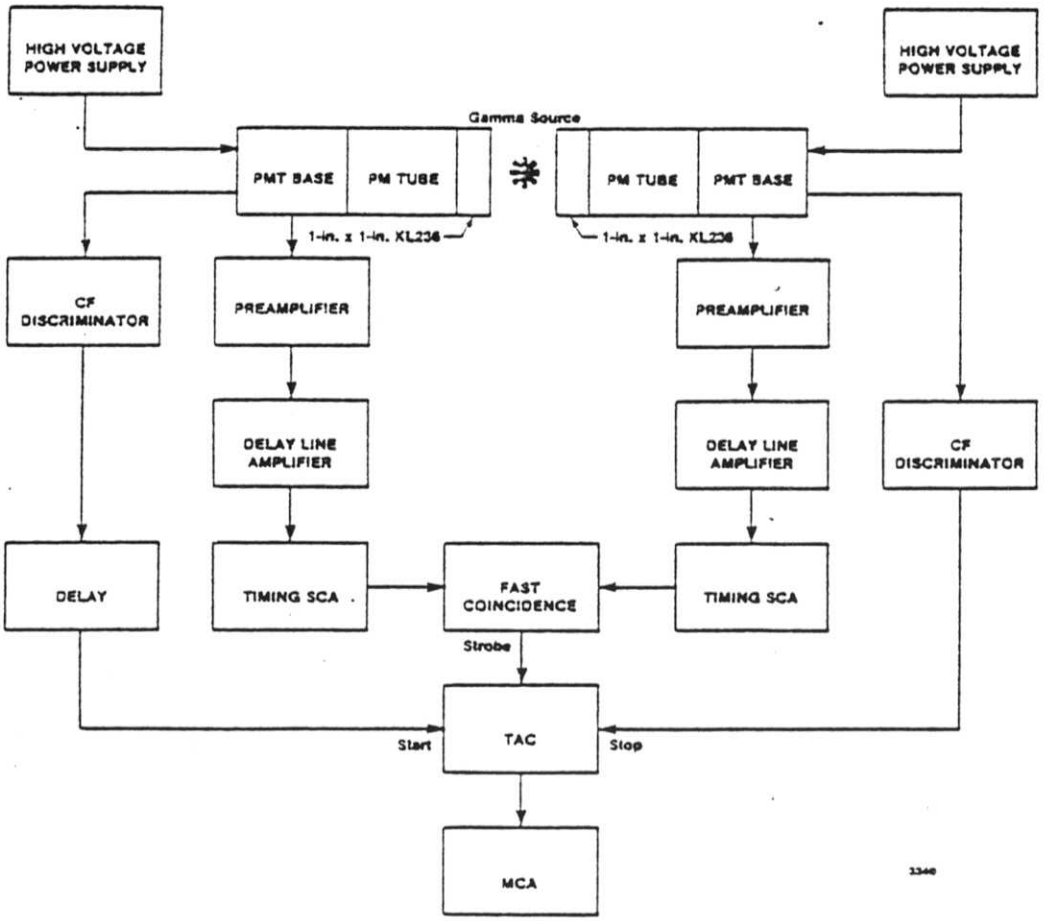

Fig 12. Typical Fast/Slow Timing System for Gamma-Gamma Coincidence Measurements with Scintillators and Photomultiplier Tubes.

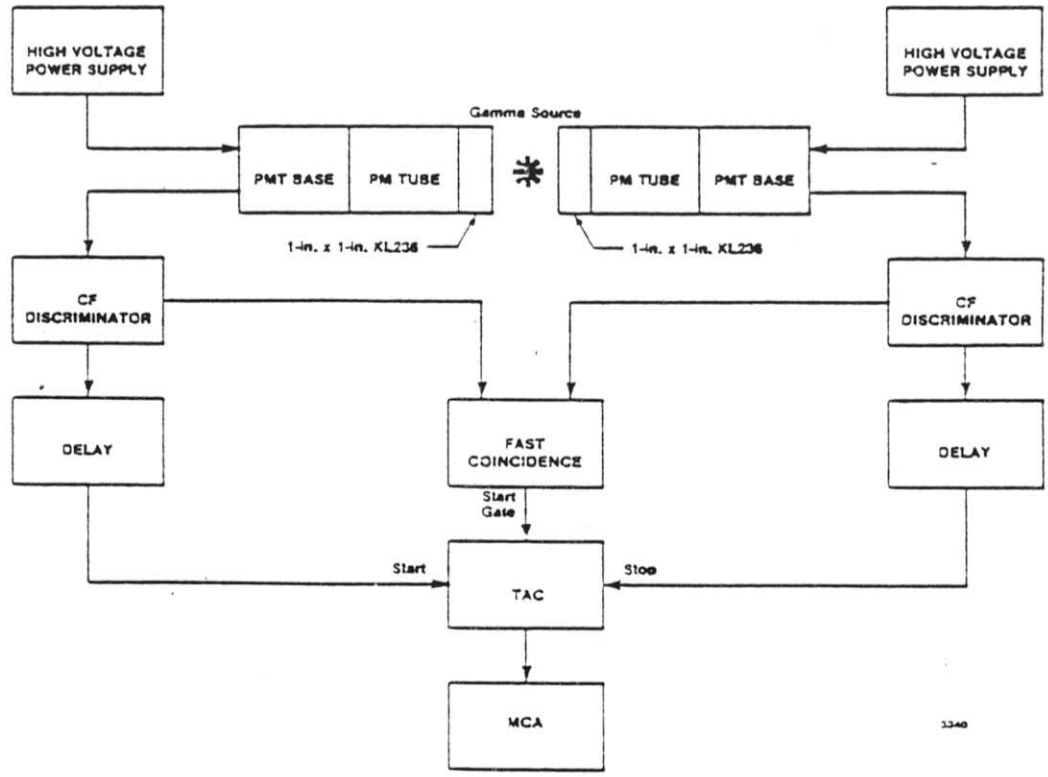

Fig 13. A Fast-Timing Concidence System for Gamma-Gamma Coincidence Measurements with Scintillators and Photomultiplier Tubes.

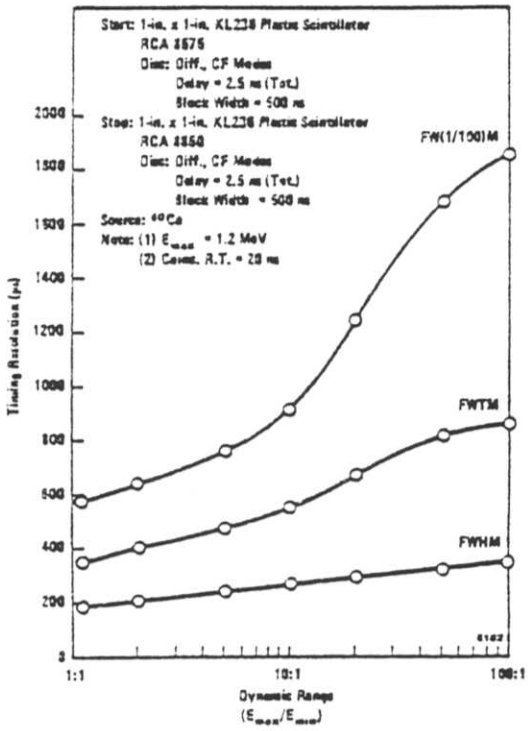

Fig 14. Timing Resolution as a Function of Dynamic Range for Two Constant-Fraction Differential Discriminators in a Fast Timing System.

VII. REFERENCES

Due to space limitations, no attempt will be made to form a complete and comprehensive bibliography in this paper. However, Ref 1 is available on request and contains over 110 references to form a starting point for a detailed bibliography on timing spectroscopy. The interested reader should consult the IEEE Trans. on Nucl. Sci., Nuclear Inst. and Meth., and Review of Sci. Inst. to remain abreast of the current trends in timing spectroscopy. The following list of references is intended only to support specific points within this paper.

1. T. J. Paulus, "Principles and Applications of Timing Spectroscopy," Application Note AN-42, EG&G ORTEC, Oak Ridge, TN 37830, (1982).

2. D. A. Gedcke and W. J. McDonald, "A Constant Fraction of Pulse Height Trigger for Optimum Time Resolution," Nucl. Inst. Methods 55, 377 (1967).

3. Z. H. Cho and R. L. Chase, "Improved Amplitude and Rise Time Compensated Timing with Ge Detectors," IEEE Trans. Nucl. Sci. NS-19(1), 451 (1972).

4. M. R. Maier and P. Sperr, "On the Construction of a Fast Constant Fraction Trigger with Integreated Circuits and Application to Various Photomultiplier Tubes," Nucl. Instr. Methods 87, 13 (1970).

5. M. O. Bedwell and T. J. Paulus, "A Versatile Constant Fraction 100-MHz Discriminator," IEEE Trans. Nucl. Sci. NS-25(1), 86 (1978).

6. M. O. Bedwell and T. J. Paulus, "A Constant Fraction Differential Discriminator for Use in Fast Timing Coincidence Systems," IEEE Trans. Nucl. Sci. NS-26(1), 442 (1979).

This Tutorial paper was presented at the Nuclear Science Symposium ,Oct.31-Nov.2 1984.